Japanese Journal of Applied Physics
Vol. 43, No. 11A, 2004, pp. L1449–L1451

Scanning Differential-Phase-Contrast Hard X-Ray Microscopy with Wedge Absorber Detector

Yasushi KAGOSHIMA*, Ken-ich SHIMOSE, Takahisa KOYAMA, Izumi WADA, Akihiko SAIKUBO, Kenji HAYASHI, Yoshiyuki TSUSAKA and Junji MATSUI

Graduate School of Material Science, University of Hyogo, 3-2-1 Kouto, Kamigori, Ako, Hyogo 678-1297, Japan

(Received July 28, 2004; accepted September 17, 2004; published October 15, 2004)

A new and simple idea for scanning differential-phase-contrast (S-DPC) hard X-ray microscopy has been proposed. It only uses a wedge absorber coupled with two intensity detectors, and is much more sensitive to sample structures than absorption contrast. It can also extract pure quantitative one-dimensional phase gradient given by a sample without an effect of sample absorption. The S-DPC microscope has been constructed at BL24XU of SPring-8, and its feasibility has been successfully demonstrated at the photon energy of 10 keV by clearly visualizing structures of samples. Further, the experimental phase gradient profile agrees well with simulation. By integrating the resultant phase gradient, the corresponding phase shift distribution could be also imaged. [DOI: 10.1143/JJAP.43.L1449]

KEYWORDS: X-ray microscope, hard X-ray, scanning microscope, zone plate, phase contrast, differential phase contrast, synchrotron radiation, phase gradient, phase shift

There are two main types in X-ray microscopes, one is an imaging type and the other is a scanning type.[1] The former provides direct magnification and shorter exposure time, while the latter provides digitally stored images with minimal radiation exposure to samples.[1] Recently, phase-contrast X-ray microscopy has rapidly grown in the hard X-ray region since the advent of the 3rd generation synchrotron radiation facilities. It is based on the fact that phase-shift cross section is almost a thousand times larger than absorption one for light elements as expected from a comparison between real and imaginary parts of the refractive index.[2,3] In the imaging type, the phase-contrast microscopy has been demonstrated by the Zernike's method[4,5] and the differential interference contrast method.[6] Further, we have recently demonstrated the novel imaging phase-contrast microscopy using a micro-interferometer consisting of a twin zone plate.[7] On the other hand, in the scanning type, the phase-contrast microscopy has been demonstrated by the configured[8] or segmented[9] detectors, the CCD-camera image-detections,[10–12] the diffracting aperture based method[13] and the dark-field imaging.[14,15] The former two require the highly sophisticated X-ray detector of electronic devises. The CCD-camera image-detection must take diffraction images of a microbeam for all pixels, thus need a huge memory and the stored dataset must be processed later with an appropriate numerical calculation for image reconstruction. The diffracting aperture based method and the dark-field imaging are simple methods to realize the scanning phase-contrast microscopy, but phase information was not evaluated quantitatively.

Here, we propose a new idea for S-DPC hard X-ray microscopy. It is a very simple way to purely extract quantitative one-dimensional phase gradient given by a sample to be imaged removing an effect of sample absorption by only adding a wedge absorber coupled with two intensity detectors into the normal scheme of the scanning microscopy. In this paper, the concept of the S-DPC hard X-ray microscopy is described and the feasibility test is presented.

The principle of the S-DPC microscopy is illustrated in Fig. 1. The optical arrangement is completely the same as the normal scheme of absorption-contrast scanning microscopy using a zone plate as a focusing X-ray lens except for a wedge absorber and an intensity detector placed in the most downstream. Two ion chambers (IC0 and IC1), which can pass a beam, are essential, and absorption-contrast images can be obtained with the two ion chambers. Here, a PIN photodiode is used as the downstream intensity detector. It should be noted that a refraction angle θ caused by a sample is very small because a refraction index of samples composed of light elements is almost equal to unity in the hard X-ray region, and therefore approximations of $\sin\theta \sim \theta$ and $\tan\theta \sim \theta$ hold. Further, since numerical aperture of a zone plate is also small, the focusing beam may be treated as a parallel beam. The IC0 measures incident X-rays intensity (I_0) and used for intensity normalization. The IC1 measures transmitted intensity (I_1) through the sample. Therefore, two-dimensional sample transmission $T_s(x, y)$ can be calculated easily as the following equation.

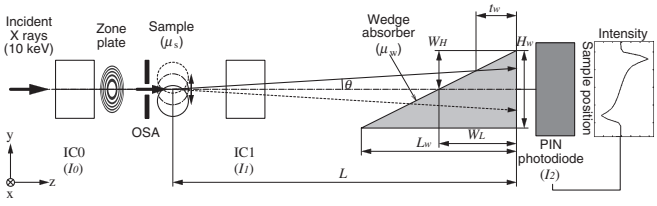

Fig. 1. Schematic illustration of proposed S-DPC hard X-ray microscope. The change of a refraction angle caused by a sample can be converted into the change of intensity by using a wedge absorber coupled with two intensity monitors (I_1 and I_2). μ_s and μ_w are linear absorption coefficient of the sample and the wedge absorber material, respectively.

$$T_s(x, y) = \frac{I_1}{I_0} = e^{-\int \mu_s(x,y,z)dz}, \quad (1)$$

where $\mu_s(x, y, z)$ is linear absorption coefficient of the sample and a direction of the incident beam is taken to be parallel to the z-axis. $T_s(x, y)$ corresponds to the absorption-contrast image. Neglecting absorption in air, path length inside the wedge absorber t_w can be expressed as

*E-mail address: kagosima@sci.u-hyogo.ac.jp

$$t_w = \frac{1}{\mu_w} \ln\left(\frac{I_1}{I_2}\right), \quad (2)$$

where μ_w is linear absorption coefficient of the wedge absorber material. When the beam is refracted upward as a solid line in Fig. 1, t_w becomes small, while when the beam is refracted downward as a dashed line in Fig. 1, t_w becomes large. Thus, a change of θ can be converted to a change of t_w. From eq. (2), t_w can be obtained independently from sample absorption by measuring transmitted intensity (I_2) through the wedge absorber. Therefore, the refraction angle θ can be easily calculated from t_w by

$$\theta \sim \frac{W_H}{L}\left(1 - \frac{t_w}{W_L}\right), \quad (3)$$

which is simply derived by similarity of a triangle geometry. W_H and W_L can be determined by measuring intensities I_1 and I_2 without a sample. The refraction angle θ is represented by

$$\theta = \frac{1}{k}\left(\frac{\partial\phi}{\partial y}\right), \quad (4)$$

where k is a wave number of the incident X-rays and $\partial\phi/\partial y$ is a phase gradient in the y-direction we are going to reveal as the differential-phase-contrast. In the above considerations, it is assumed that the refraction index of the wedge absorber material is very near to unity, and thus the refraction can be neglected when the X-rays are incident into the wedge absorber.

The S-DPC microscope has been constructed at BL24XU[16] of SPring-8. The photon energy of the fundamental harmonic peak of the undulator was tuned to 10 keV. The X-ray beam was horizontally collimated by a 200-μm-width slit in front of a horizontal-dispersion silicon double-crystal monochromator (111 reflection) placed 60 m apart from the undulator source point. A plane SiO_2 mirror was used to eliminate higher energy X-rays. The grazing incident angle was 0.14°. A phase zone plate made of tantalum[17] produces an X-ray microbeam. The diameter, the outermost zone width, the thickness of tantalum and the focal length at 10 keV are 100 μm, 250 nm, 2.4 μm and 202 mm, respectively. The zone plate has a 5.6-μm thick and 44.6-μm-diameter gold center stop. In order to further suppress the direct beam transmitting through the zone plate, a gold beam stopper with a thickness of 3 μm and a diameter of 20 μm was also added in front of the zone plate. A platinum 10-μm-diameter pinhole is used as an order-sorting aperture (OSA). The wedge absorber is made of teflon (C_2F_4: density = 2.2 g/cm^3; $\delta = 4.405 \times 10^{-6}$, $\beta = 1.404 \times 10^{-8}$ at 10 keV)[18] and its dimension is 2 cm (L_w) × 1 cm (H_w) × 1 cm (depth). The PIN photodiode was placed just behind the wedge absorber to measure I_2.

The focused beam size was measured by the use of a knife-edge method, and it was evaluated to be 1.7 μm in horizontal and 1.0 μm in vertical directions. A distance between the sample and the wedge absorber end (L) was 2.16 m. Since the numerical aperture of a zone plate can be written as

$$NA_{ZP} = \frac{\lambda}{2\delta r_N}, \quad ^{1)}$$

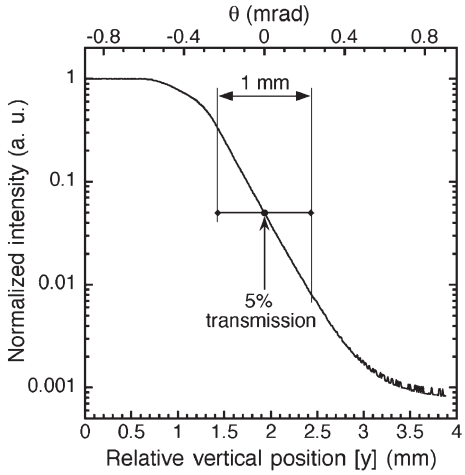

Fig. 2. y (θ) - log[normalized I_2] curve measured by moving the wedge absorber in the vertical direction without a sample. Coverable range of the refraction angle θ was estimated to be ±230 μrad when the wedge absorber was fixed at the position giving the transmission of 5%.

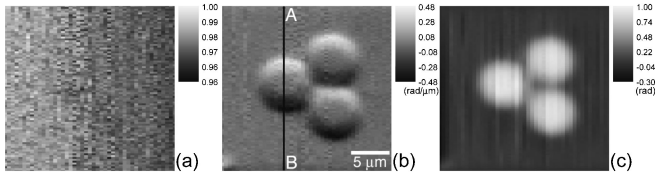

Fig. 3. S-DPC images of 7-μm-diameter polystyrene micro-particles; (a) absorption-contrast, (b) differential-phase-contrast and (c) phase shift distribution images, respectively. Pixel size, pixel number and acquisition time were 0.5 μm (x) × 0.25 μm (y), 45 (x) × 90 (y) pixels, and 0.4 s/pixel, respectively. The labels are of transmission in (a), phase gradient $\partial\phi/\partial y$ [rad/μm] in (b) and phase shift ϕ [rad] in (c), respectively.

where λ is a wavelength and δr_N is the outermost zone width, a full angular divergence of the focused beam is 500 μrad at 10 keV. Thus, the beam size at the wedge absorber end was 1.08 mm in diameter.

In order to define an acceptable range of the refraction angle θ, I_2 was measured without a sample by moving the wedge absorber in the vertical direction. The vertical position (y) can be easily converted to θ using $y \sim L\theta$. The result is shown in Fig. 2. According to eqs. (2) and (3), θ is proportional to $\ln(I_2)$. It was confirmed that the linearity could be conserved within ±0.5 mm in y, which corresponded to ±230 μrad in θ, when the wedge absorber was fixed at the position giving the transmission of 5%. According to eq. (4), the coverable phase gradient ($\partial\phi/\partial y$) range is within ±11.7 rad/μm. The 5% transmission corresponded that t_w was 2.11 mm, and thus W_L was 2.11 mm and W_H was 1.05 mm.

As a transparent sample, 7-μm-diameter polystyrene micro-particles were observed. Figures 3(a) and 3(b) show absorption-contrast and differential-phase-contrast images, respectively. The sample structures can never be seen in Fig. 3(a) as expected from calculated transmission of 99.8%, while the three particles can be clearly observed in Fig. 3(b). The results demonstrate that the present S-DPC microscopy possesses sensitivity high enough to visualize microstructures of transparent samples. Analyzing background signals

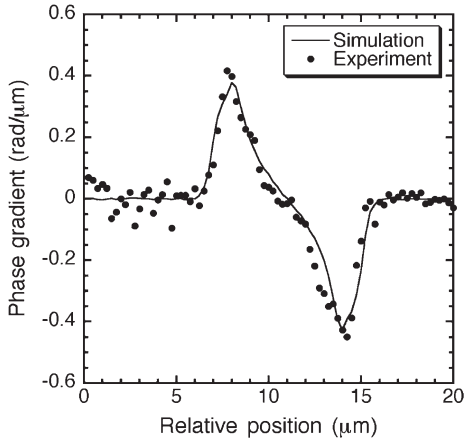

Fig. 4. Comparison between simulation and the experimental phase gradient profile along line A-B in Fig. 3(b). A solid line and dots are the simulation and experimental results, respectively. They show good agreement with each other.

of Fig. 3(b), the minimum detectable phase gradient could be estimated to be as small as 0.1 rad/μm under the assumption that it is defined as 3 times of standard deviation of background signals. The phase gradient of 0.1 rad/μm corresponds to the very small refraction angle of 2.0 μrad according to eq. (4).

The experimental phase gradient profile was compared to simulation of ray tracing. The simulation was carried out assuming the same optical setup shown in Fig. 1. The sample was assumed to be a 7-μm-diameter polystyrene ($\delta = 2.440 \times 10^{-6}$)[18] sphere. The incident beam consisting of many rays was assumed to have a Gaussian intensity profile with a beam size of 1.0 μm in FWHM and to have a rectangular angular profile with a full divergence of 500 μrad. The sample being scanned, the refraction angle of each ray was calculated according to the law of refraction, and then I_2 was calculated at each sample position. Total reflection condition was also taken into account, though the effect was negligible. Finally the phase gradient was calculated using the same procedure as the experimental data handling. The simulation result and the experimental phase gradient profile along the line A-B in Fig. 3(b) are shown in Fig. 4. They show good agreement with each other, and thus it was confirmed that the present S-DPC microscopy could provide not only highly sensitive sample structures but also quantitative information of the phase gradient. Furthermore, by integrating phase gradient values in Fig. 3(b) along y-axis, phase shift distribution can be also imaged as shown in Fig. 3(c). A 7-μm-thick polystyrene ($t = 7\,\mu m$) gives the phase shift [$\phi = (2\pi/\lambda)\delta t$] of 0.87 rad at 10 keV, which agrees well with the experimental values shown in Fig. 3(c).

As mentioned above, one of the merits of the present S-DPC microscopy is that differential-phase-contrast images

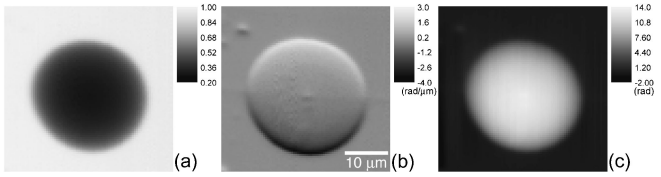

Fig. 5. S-DPC images of a 30-μm-diameter BaO-SiO_2-TiO_2 glass bead; (a) absorption-contrast, (b) differential-phase-contrast and (c) phase shift distribution images, respectively. Pixel size, pixel number and acquisition time were 0.5 μm (x) × 0.5 μm (y), 80 (x) × 80 (y) pixels, and 0.5 s/pixel, respectively.

can be obtained without an effect of sample absorption. As an absorbing sample, a 30-μm-diameter BaO-SiO_2-TiO_2 glass bead of which density is 4.1 g/cm^3 was observed. Figures 5(a), 5(b) and 5(c) show absorption-contrast, differential-phase-contrast and phase shift distribution images, respectively. In Fig. 5(a), the minimum transmission is as small as 20%. Nevertheless, any effects due to absorption cannot be seen in Fig. 5(b). Thus, it was also confirmed that the present S-DPC microscopy could extract pure phase gradient removing the effect of sample absorption.

This work has been carried out according to the SPring-8 proposal number of C03B24XU-5042N.

1) J. Kirz and H. Rarback: Rev. Sci. Instrum. **56** (1985) 1.
2) A. Momose and J. Fukuda: Med. Phys. **22** (1995) 375.
3) A. Momose, T. Takeda, Y. Itai and K. Hirano: Nature Med. **2** (1996) 473.
4) Y. Kagoshima, T. Ibuki, Y. Yokoyama, Y. Tsusaka, J. Matsui, K. Takai and M. Aino: Jpn. J. Appl. Phys. **40** (2001) L1190.
5) U. Neuhäusler, G. Schneider, W. Ludwig and D. Hambach: J. Phys. IV France **104** (2003) 567.
6) T. Wilhein, B. Kaulich, E. Di Fabrizio, F. Romanato, S. Cabrini and J. Susini: Appl. Phys. Lett. **78** (2001) 2082.
7) T. Koyama, Y. Kagoshima, I. Wada, S. Saikubo, K. Shimose, K. Hayashi, Y. Tsusaka and J. Matsui: Jpn. J. Appl. Phys. **43** (2004) L421.
8) G. R. Morrison: Proc. SPIE **1741** (1992) 186.
9) M. Feser, C. Jacobsen, P. Rehak and G. DeGeronimo: J. Phys. IV France **104** (2003) 529.
10) H. N. Chapman, C. Jacobsen and S. Williams: Rev. Sci. Instrum. **66** (1995) 1332.
11) G. R. Morrison and B. Niemann: in *X-Ray Microscopy and Spectromicroscopy*, eds. J. Thieme, G. Schmahl, D. Rudolph and E. Umbach (Springer-Verlag, Berlin, 1998) p. I-85.
12) H. Takano, K. Uesugi, A. Takeuchi, K. Takai and Y. Suzuki: J. Phys. IV France **104** (2003) 41.
13) B. Kaulich, F. Polack, U. Neuhäusler, J. Susini, E. Di Fabrizio and T. Wilhein: Optics Express **10** (2002) 1111.
14) G. R. Morrison and M. Browne: Rev. Sci. Instrum. **63** (1992) 611.
15) Y. Suzuki and F. Uchida: Rev. Sci. Instrum. **66** (1995) 1468.
16) Y. Tsusaka, K. Yokoyama, S. Takeda, K. Takai, Y. Kagoshima and J. Matsui: Nucl. Instrum. & Methods A **467–468** (2001) 670.
17) A. Ozawa, T. Tamamura, T. Ishii, H. Yoshihara and Y. Kagoshima: Microelectron. Eng. **35** (1997) 525.
18) B. L. Henke, E. M. Gullikson and J. C. Davis: At. Data & Nucl. Data Tables **54** (1993) 181.